*A joint special edition on*

# Sources and Sinks of Ocean Mesoscale Eddy Energy

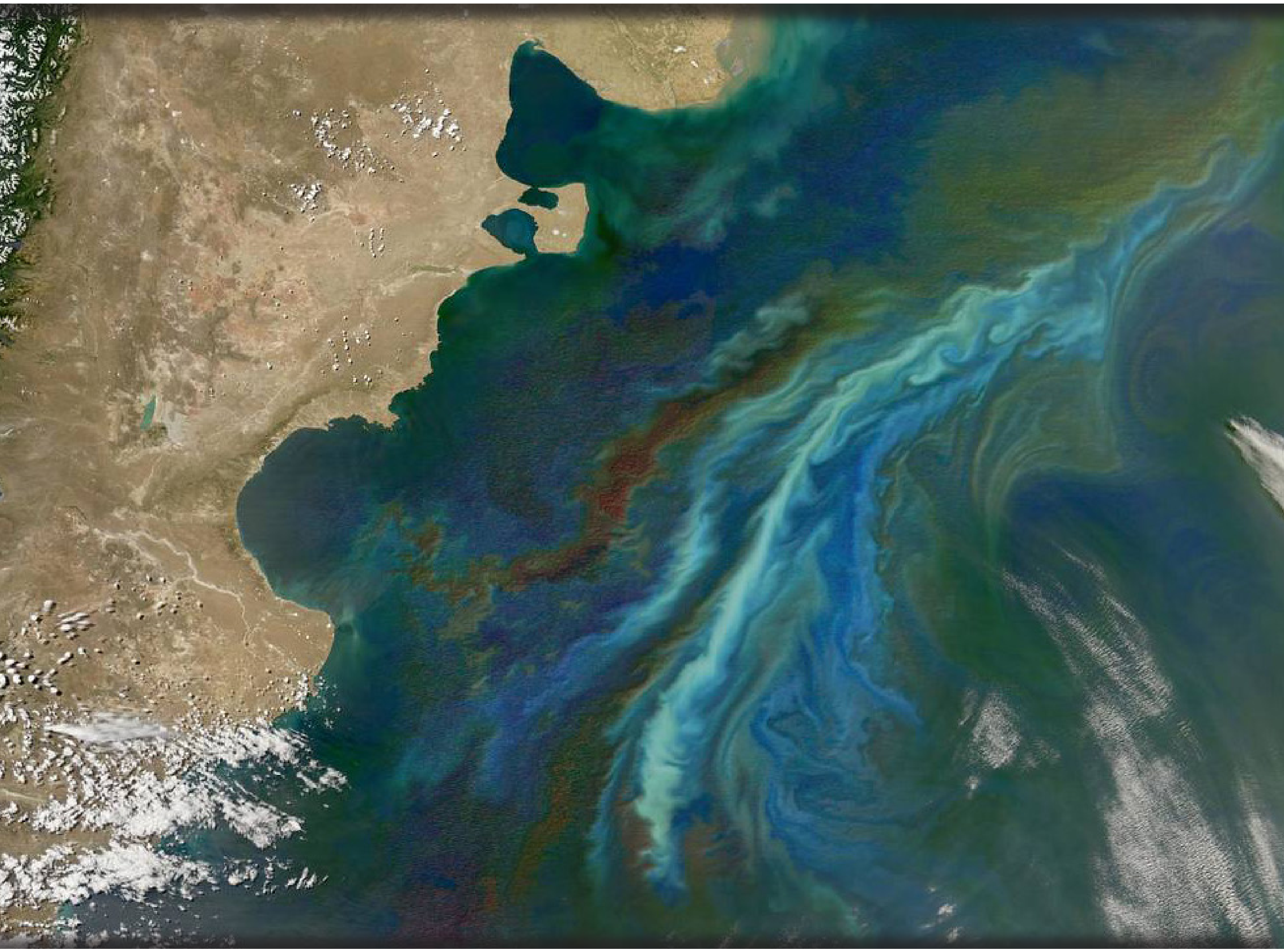

*Image credit: NASA Earth Observatory*

CLIVAR *Exchanges*
No. 77 • February 2020
ISSN No: 1026-0471

US CLIVAR *Variations*
Winter 2020 • Vol. 18, No. 1
DOI: 10.5065/g8w0-fy32

# Impact of horizontal resolution on the energetics of global ocean−sea-ice model simulations

**Eric P. Chassignet[1], Stephen G. Yeager[2], Baylor Fox-Kemper[3], Alexandra Bozec[1], Frederic S. Castruccio[2], Gokhan Danabasoglu[2], Who M. Kim[2], Nikolay Koldunov[4], Yiwen Li[5], Pengfei Lin[5], Hailong Liu[5], Dmitry Sein[4,6], Dmitry Sidorenko[4], Qiang Wang[4], and Xiaobiao Xu[1]**

[1]Florida State University, US

[2]National Center for Atmospheric Research, US

[3]Brown University, US

[4]Alfred-Wegener-Institut Helmholtz-Zentrum für Polar- und Meeresforschung (AWI), Germany

[5]Chinese Academy of Sciences, China

[6]Shirshov Institute of Oceanology, Russian Academy of Science, Russia

In order to investigate the origins and consequences of systematic ocean-sea-ice model biases in climate models, an international group of ocean modelers proposed an Ocean Model Intercomparison Project (OMIP; Griffies et al. 2016). The essential element behind the OMIP is a common set of atmospheric and river runoff datasets for computing surface boundary fluxes to drive the ocean-sea-ice models, many of which are used as components of coupled climate system models. The OMIP protocol is an outcome of the Coordinated Ocean-ice Reference Experiments (CORE), which assessed the performance of ocean-sea-ice models (Griffies et al. 2009; Danabasoglu et al. 2014; Griffies et al. 2014; Downes et al. 2015; Farneti et al. 2015; Danabasoglu et al. 2016; Wang et al. 2016a, 2016b; Ilicak et al. 2016; Tseng et al. 2016; Rahaman et al. 2020) using the atmospheric and river runoff dataset of Large and Yeager (2009). However, this dataset has not been updated since 2009 and a new dataset (JRA55-do; Tsujino et al. 2018) has been developed for the OMIP based on the Japanese Reanalysis (JRA-55) product from Kobayashi et al. (2015) to ensure that it is regularly updated. Tsujino et al. (2020) compares CORE-forced (i.e., OMIP-1) and JRA55-do-forced (i.e., OMIP-2) simulations considering metrics commonly used in the evaluation of global ocean-sea-ice models to assess model biases. Many features are very similar between OMIP-1 and OMIP-2 simulations, but Tsujino et al. (2020) identify many improvements in the simulated fields in transitioning from OMIP-1 to OMIP-2. They attribute many of the remaining model biases either to errors in representing important processes in ocean-sea-ice models (some of which are expected to be mitigated by taking finer horizontal and/or vertical resolutions) or to shared biases in the atmospheric forcing. A first attempt at quantifying the impacts of the models' horizontal resolution on biases was made by Chassignet et al. (2020). They assess the robustness of climate-relevant improvements in ocean simulations (mean and variability) associated with moving from coarse (~1º) to eddy-resolving (~0.1º) horizontal resolutions using the same atmospheric forcing dataset (JRA55-do) for both low- and high-resolution configurations. Within the ocean modeling community, it is usually assumed that high-resolution simulations should in general produce better results than low-resolution ones (Fox-Kemper et al. 2019). While this is clearly the case for surface currents and internal variability, greatly enhanced horizontal resolution does not necessarily deliver unambiguous bias improvement in temperature and salinity in all regions (Chassignet et al. 2020). Here, we emphasize some of the salient points of Chassignet et al. (2020) most relevant to the main topic of this special joint issue of US CLIVAR Variations and CLIVAR Exchanges., i.e., "Sources and Sinks of Ocean Mesoscale Eddy Energy."

Because the goal is to identify the robust differences and improvements associated with increased horizontal resolution given the same forcing datasets, the participating modeling groups configured their high-resolution configuration with similar parameters to that of the coarse-resolution configuration (see Chassignet et al. 2020 for details). The four models that participated in the comparison are the HYbrid Coordinate Ocean Model (HYCOM, Bleck 2002; Chassignet et al. 2003), the ocean (POP) and sea-ice components of the Community Earth System Model version 2 (CESM2, Danabasoglu et al. 2020), the ocean-sea ice component (FESOM) of the coupled Alfred Wegener Institute Climate Model (AWI-CM, Sidorenko et al. 2015, 2018; Rackow et al. 2018, 2019; Sein et al. 2018), and the LASG/IAP Climate system Ocean Model (LICOM, Zhang et al. 1989; Liu et al. 2004; Liu et al. 2012; Yu et al. 2018; Lin et al. 2020). Because of the large computational cost associated with the high-resolution runs (factor of 1000 more expensive), only one JRA55-do cycle (1958-2018) is analyzed (versus six cycles for the coarse-resolution runs of Tsujino et al. 2020). It is important to note that not all models use the same climatology for the initial conditions, nor do they use the same wind stress formulation (absolute versus relative winds). When evaluating the bias of a numerical simulation, it is performed with respect to the climatology used to initialize the run.

Table 1 shows the domain-averaged mean kinetic energy for all experiments averaged over the last 20 years of the 1958 -2018 integrations. Not surprisingly, the total kinetic energy is significantly higher for the high-resolution experiments over the low-resolution experiments. For the high-resolution configurations, HYCOM has the highest kinetic energy, with a globally averaged value of ~35 $10^{-4}$ $m^2/s^2$ and LICOM has the lowest kinetic energy, with a globally averaged value of ~15 $10^{-4}$ $m^2/s^2$ (Table 1). The higher kinetic energy in HYCOM can be partially explained by the wind stress formulation, which does not take into account the ocean current velocities (absolute winds) while the other three models do (relative winds). The latter has an eddy killing effect that can reduce the total kinetic energy by as much as 30% (see Renault et al.

**Table 1.** Global mean kinetic energy per surface area (units are in $10^{-4}$ $m^2/s^2$).

| | Low-resolution | High-resolution |
|---|---|---|
| HYCOM | 11 | 36 |
| NCAR | 6 | 24 |
| FESOM | 9 | 19 |
| LICOM | 4 | 14 |

2019 for a review). This is roughly the difference that is seen here between HYCOM and POP (POP with absolute winds in the wind stress has a level of kinetic energy that is close to HYCOM in Maltrud and McClean 2005, see their Figure 1). But even with the highest resolution used here (~0.1°), the total kinetic energy remains significantly lower than what can be inferred from observations and higher resolution models (closer to $50\ 10^{-4}\ m^2/s^2$, i.e., Chassignet and Xu 2017). The increase in total kinetic energy from the low- to the high-resolution configuration is approximately a factor of three to four for all models, except for FESOM (factor two only). This is probably because the high-resolution FESOM has a highly variable grid spacing (Chassignet et al. 2020) and does not resolve the Rossby radius of deformation everywhere.

The impact on the circulation of increasing the horizontal resolution is two-fold. First, the solution becomes more nonlinear and allows for a better representation of western boundary currents. Second, the first Rossby radius of deformation is resolved throughout most of the domain (Hallberg 2013) and eddies are formed through barotropic and baroclinic instabilities, although higher vertical modes including submesoscale eddies are not often resolved (nor are they resolved by altimetry, i.e. AVISO). Overall, the large-scale patterns are well represented globally, and there is a significant improvement in the representation of the western boundary currents as resolution is increased (Gulf Stream and Kuroshio). In the North Atlantic, most coarse resolution models to date have the tendency to exhibit

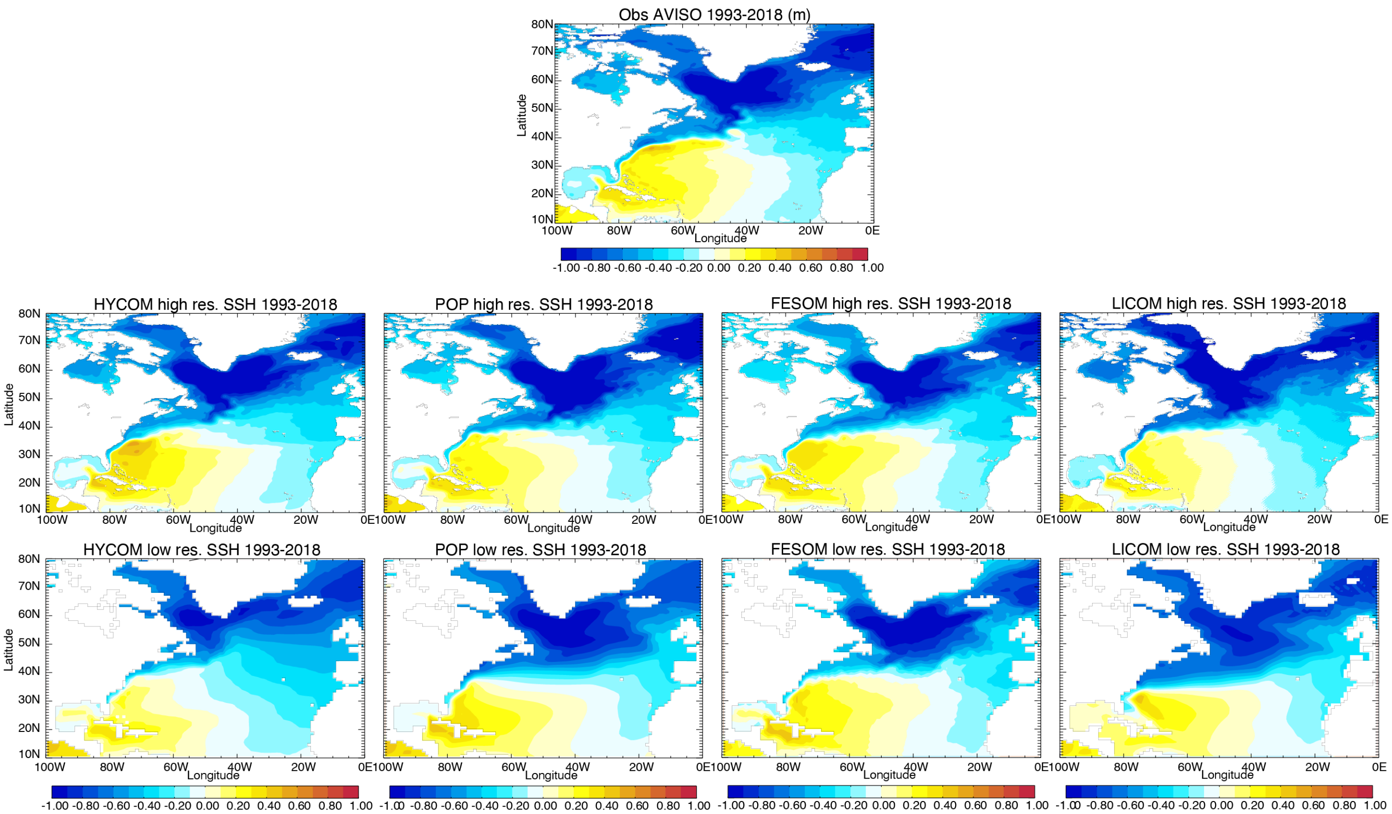


**Figure 1.** Mean sea surface height fields for observations (Rio et al. 2014) (top panel), high-resolution experiments (middle panel), and low-resolution experiments (lower panel).

an overshooting Gulf Stream and a poor representation of the North Atlantic Current (NAC) at the Northwest Corner (Figure 1). This was the case for three out of the four models. Instead of turning north-northeastward along the continental rise of the Grand Banks and past the Flemish Cap to a latitude of ~51°N before turning eastward (see review paper by Rossby 1996), the modeled NAC is strongly zonal in POP, FESOM, and LICOM, and does not turn northward near the Grand Banks (Figure 1). This has been a long-standing issue for many ocean components of the CMIP climate models, and it does not necessarily improve as the computational mesh is refined. Increasing the horizontal resolution does improve the Gulf Stream separation (see Chassignet and Marshall 2008 and Chassignet and Xu 2017 for a review) in all models, but not necessarily the representation of the Northwest Corner circulation. HYCOM is the only model that had a good representation of the Northwest Corner in both the low- and high-resolution experiments (Figure 1). Since all the models use the same atmospheric forcing dataset, the difference is solely due to the numerical and physical choices made by each modeling group.

As expected, there is a significant increase in the sea surface height (SSH) variance as resolution increased and the eddying solution SSH variance maps are much closer to the observations than their low-resolution counterpart (Chassignet et al. 2020). The surface eddy kinetic energy (EKE) maps for two of the high-resolution simulations (HYCOM and POP) and from observations (AVISO) are displayed in Figure 2. The AVISO EKE map has some inherent smoothing since the along-track measurements were optimally interpolated on a 0.25° grid which filters scales less than 150 km (due to track separation and measurement noise and errors) and time scales less than 10 days (repeat cycle of the altimeters). To match the observations, the modeled EKE maps are computed using 10-day average outputs and this time averaging removed much of the small-scale variability associated with inertial motions and ageostrophic effects (Chassignet and Xu 2017). Overall, the EKE is larger in HYCOM because absolute winds are used to force the models, but in all high-resolution experiments (~0.1°), the variability is still lower than observed, especially in the gyre interiors and in the experiments that used relative winds (POP, FESOM, and LICOM). This underestimation is thus partly a consequence of the eddy-killing effect which results from considering the shear between atmospheric wind and ocean current when computing the wind stress, which can reduce the kinetic energy by as much as 30% (see above discussion). However, the use of absolute wind in HYCOM is not sufficient to raise the level of surface variability to that of the observations, and Chassignet and Xu (2017) argue that one actually needs to significantly increase the resolution (~0.01°) in order to resolve the submesoscale instabilities that can energize the mesoscale (Callies et al. 2016) and therefore enhance EKE comparable to the mesoscale AVISO observations. It is more physical to take into account the vertical shear between atmospheric winds and ocean currents when computing the wind stress (see Renault et al. 2019, for a review), as it allows for a better representation of western boundary current systems (Ma et al. 2016), especially the Agulhas Current retroflection and associated eddies (Renault et al. 2017). In HYCOM, the Agulhas eddies are too regular and follow the same pathway (Figure 2). The use of relative winds does improve the pathway for the Agulhas current eddies (NCAR vs. HYCOM), but it also reduces the level of EKE in the Antarctic Circumpolar Current (ACC) and suppresses variability in many areas. This is especially true for the Indian Ocean, in the tropics, and west of the Hawaiian Islands. Most model-observations comparisons usually focus on the surface fields because of the scarcity of long time series at depth covering a large spatial area. While the EKE at depth in the high-resolution experiments is a significant improvement over the quasi non-existent EKE of the coarse-resolution simulations, it is still significantly less than very limited observations (Richardson, 1993; Ollitrault and Colin de Verdière 2014). There is however much less EKE at depth in the experiments using relative winds (POP, FESOM, or LICOM) than in the experiment using absolute winds (HYCOM, not shown). Significantly higher resolution may be necessary in order to obtain a level of EKE at depth close to the observations (see Chassignet and Xu 2017 for a discussion).

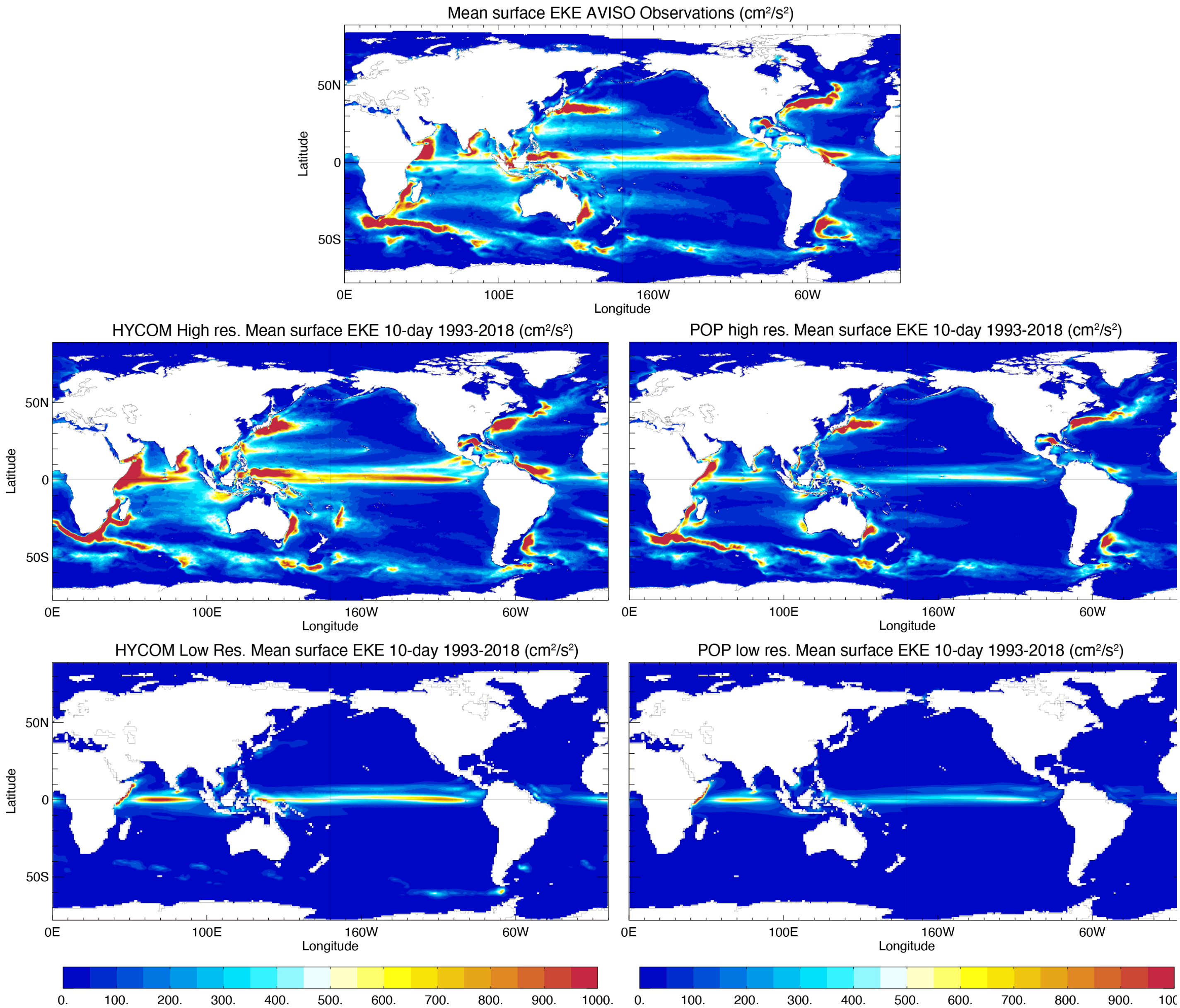


**Figure 2.** Mean surface eddy kinetic energy for observations (top panel), high-resolution experiments (middle panel), and low-resolution experiments (lower panel).

Overall, the gross features of the bias patterns in low resolution models – position, strength, and variability of western boundary currents, equatorial currents, and ACC – are significantly improved in the high-resolution models. However, despite the fact that the high-resolution models "resolve" these features, the improvements in temperature or salinity are inconsistent among different model families and some regions show increased bias over their low-resolution counterparts (see Chassignet et al. 2020 for a discussion). SSH variability and near-surface EKE are significantly – even qualitatively – improved in all high-resolution models over their low-resolution counterparts, although all of these models still underpredict the observed SSH variability and EKE, particularly in the ocean interior, which indicates a need for further refinements in resolution (Chassignet and Xu 2017) and improvements in less dissipative subgrid schemes for high-resolution models (Pearson et al. 2017). The results in coupled models in the HighResMIP ensemble (Haarsma et al. 2016) show similar improvements in SSH and SST variability and EKE. Considerable differences in the high-resolution models used here are associated with the use of relative winds versus absolute winds.

Another interesting aspect of the high-resolution models versus the low-resolution models is that the interannual variability in the ACC, Indonesian Throughflow, and Atlantic Meridional Overturning Circulation (AMOC) transports (not shown) is more consistent among the high-resolution models than among the low-resolution models (Chassignet et al. 2020). Consistency in all of these transports potentially indicates that higher-resolution models are needed to represent process variability, which may explain some of the past difficulties in comparing the magnitude of these phenomena across coarse-resolution models. However, the mean ACC transport and AMOC strength are not in greater agreement among the high-resolution than the low-resolution models, which means that more work remains in evaluating sensitivity to numerics and subgrid-scale schemes for high-resolution models. Furthermore, Danabasoglu et al. (2016) note that low-resolution models come into greater agreement in AMOC variability after more cycles of the CORE forcing. This comparison is limited by the cost of the high-resolution models to only a single cycling of the forcing. The short duration of a single forcing cycle limits the comparison of the decadal changes that are emphasized in Danabasoglu et al. (2016), so the improved agreement among the high-resolution models is year-by-year rather than decade-by-decade. Nonetheless, the high-resolution models have systematically stronger and more variable AMOC, in better agreement with observations, both in maximum overturning and profile, than the low-resolution models.

*Acknowledgements*
The HYCOM contribution was supported by the National Oceanic and Atmospheric Administration (NOAA) Earth System Prediction Capability Project (Award NA15OAR4320064), NOAA Modeling, Analysis, Predictions and Projections (MAPP) Program (Award 5NA15OAR4310088), and National Science Foundation (NSF) Physical Oceanography Program (Award 1537136). The POP contribution was supported by the NOAA Climate Variability and Predictability (CVP) Program. NCAR is a major facility sponsored by the NSF under Cooperative Agreement No. 1852977. The FESOM contribution was supported by the projects S1 (Diagnosis and Metrics in Climate Models) and S2 (Improved Parameterizations and Numerics in Climate Models) of the Collaborative Research Centre TRR 181 "Energy Transfer in Atmosphere and Ocean" funded by the Deutsche Forschungsgemeinschaft (DFG, German Research Foundation) – Project No. 274762653, Helmholtz Climate Initiative REKLIM (Regional Climate Change) and European Union's Horizon 2020 Research & Innovation programme through Ggrant Aagreement No. 727862 APPLICATE. The LICOM contribution was supported by the National Natural Science Foundation of China (Grants No. 41931183 and 41976026). D. Sein was supported by the state assignment of FASO Russia (theme 0149-2019-0015).

*References*

Bleck, R., 2002: An oceanic general circulation model framed in hybrid isopycnic-Cartesian coordinates. *Ocean Modell.*, **37**, 55-88, doi:10.1016/S1463-5003(01)00012-9.

Callies, J., G. Flierl, R. Ferrari, and B. Fox-Kemper, 2016: The role of mixed-layer instabilities in submesoscale turbulence. *J. Fluid Mech.*, **788**, 5-41, doi:10.1017/jfm.2015.700.

Chassignet, E. P., L. T. Smith, G. T. Halliwell, and R. Bleck, 2003: North Atlantic simulations with the Hybrid Coordinate Ocean Model (HYCOM): Impact of the vertical coordinate choice, reference pressure, and thermobaricity. *J. Phys. Oceanogr*, **33**, 2504-2526, doi:10.1175/1520-0485(2003)033<2504:NASWTH>2.0.CO;2.

Chassignet, E. P., and D. P. Marshall, 2008: Gulf Stream separation in numerical ocean models. *Ocean Modeling in an Eddying Regime*, *Geophys. Monogr.,* 177, AGU Geophys. Union, 39-62.

Chassignet, E. P., and X. Xu, 2017: Impact of horizontal resolution (1/12° to 1/50°) on Gulf Stream separation, penetration, and variability. *J. Phys. Oceanogr*., **47**, 1999-2021, doi:10.1175/JPO-D-17-0031.1.

Chassignet, E. P., and Coauthors, 2020: Impact of horizontal resolution on global ocean-sea-ice model simulations based on the experimental protocols of the Ocean Model Intercomparison Project phase 2 (OMIP-2). *Geo. Model Dev.,* Submitted.

Danabasoglu, G., and Coauthors, 2014: North Atlantic simulations in Coordinated Ocean-ice Reference Experiments phase II (CORE-II). Part I: Mean states. *Ocean Modell.*, **73**, 76–107, doi:10.1016/j.ocemod.2013.10.005.

Danabasoglu, G., and Coauthors, 2016: Part I.: North Atlantic simulations in Coordinated Ocean-ice Reference Experiments phase II (CORE-II). Part II: Inter-annual to decadal variability. *Ocean Modell.*, **97**, 65–90, doi:10.1016/j.ocemod.2015.11.007.

Danabasoglu, G., and Coauthors, 2020: Community Earth System Model version 2 (CESM2). *J. Adv. Model. Earth Syst.,* Submitted.

Downes, S. M., and Coauthors, 2015: An assessment of Southern Ocean water masses and sea ice during 1988–2007 in a suite of interannual CORE-II simulations. *Ocean Modell.,* **94**, 67–94, doi:10.1016/j.ocemod.2015.07.022.

Farneti, R., and Coauthors, 2015: An assessment of Antarctic Circumpolar Current and Southern Ocean meridional overturning circulation during 1988–2007 in a suite of interannual CORE-1125 II simulations. *Ocean Modell.*, **93**, 84–120, doi:10.1016/j.ocemod.2015.07.009.

Fox-Kemper, B., and Coauthors, 2019: Challenges and prospects in ocean circulation models. *Front. Mar. Sci.*, **6**, 1-29, doi:10.3389/fmars.2019.00065.

Griffies, S. M., and Coauthors, 2009: Coordinated Ocean-Ice Reference Experiments (COREs). *Ocean Modell.*, **26**, 1-46, doi:0.1016/j.ocemod.2008.08.007.

Griffies, S. M., and Coauthors, 2014: An assessment of global and regional sea level for years 1993–2007 in 1160 a suite of interannual CORE-II simulations. *Ocean Modell.,* **78**, 35–89, doi:10.1016/j.ocemod.2014.03.004.

Griffies, S. M., and Coauthors, 2016: OMIP contribution to CMIP6: experimental and diagnostic protocol for the physical component of the Ocean Model Intercomparison Project. *Geosci. Model Dev.,* **9**, 3231–3296, doi:10.5194/gmd-9-3231-2016.

Haarsma, R. J., and Coauthors, 2016: High resolution model intercomparison project (HighResMIP v1. 0) for CMIP6. *Geosci. Model Dev.*, **9**, 4185-4208, doi:10.5194/gmd-9-4185-2016.

Hallberg, R., 2013: Using a resolution function to regulate parameterizations of oceanic mesoscale eddy effects. *Ocean Modell.*, **72**, 92–103, doi:10.1016/j.ocemod.2013.08.007.

Ilicak, M., and Coauthors, 2016: An assessment of the Arctic Ocean in a suite of interannual 1195 CORE-II simulations. Part III: Hydrography and fluxes. *Ocean Modell.*, **100**, 141–161, doi:10.1016/j.ocemod.2016.02.004.

Kobayashi, S., and Coauthors, 2015: The JRA-55 reanalysis: general specifications and basic characteristics. *J. Meteor. Soc. Japan.*, **93**, 5–48, doi:10.2151/jmsj.2015-001.

Large, W. G., and S. Yeager, 2009: The global climatology of an interannually varying air-sea flux data set. *Climate Dyn.,* **33**, 341–364, doi:10.1007/s00382-008-0441-3.

Lin, P. F., and Coauthors, 2020: LICOM model datasets for the CMIP6 Ocean Model Intercomparison Project. *Adv. Atmos. Sci.*, **37**, doi:10.1007/s00376-019-9208-5.

Liu, H. L., P. F. Lin, Y. Q. Yu, and X. H. Zhang, 2012: The baseline evaluation of LASG/IAP Climate system Ocean Model (LICOM) verion 2.0. *J. Meteor. Res.*, **26**, 318-329, doi:0.1007/s13351-012-0305-y.

Liu, H. L., X. H. Zhang, W. Li, Y. Q. Yu, and R. C. Yu, 2004: An eddy-permitting oceanic general circulation model and its preliminary evaluations. *Adv. Atmos. Sci*., **21**, 675-690, doi:10.1007/BF02916365.

Ma, X., and Coauthors, 2016: Western boundary currents regulated by interaction between ocean eddies and the atmosphere. *Nature*, **535**, 533–537, doi:10.1038/nature18640.

Maltrud, E.M., and J. McClean, 2005: An eddy resolving global 1/10° ocean simulation. *Ocean Modell.*, **8**, 31-54. doi:10.1016/j.ocemod.2003.12.001.

Ollitrault, M., and A. Colin de Verdière, 2014: The ocean general circulation near 1000-m depth. *J. Phys. Oceanogr.*, **44**, 384–408, doi:10.1175/JPO-D-13-030.1.

Pearson, B., B. Fox-Kemper, S. Bachman, and F. Bryan, 2017: Evaluation of scale-aware subgrid mesoscale eddy models in a global eddy-rich model. *Ocean Modell.*, **115**, 42-58, doi:10.1016/j.ocemod.2017.05.007.

Rackow, T., H. F. Goessling, T. Jung, D. Sidorenko, T. Semmler, D. Barbi, and D. Handorf, 2018: Towards multi-resolution global climate modeling with ECHAM6-FESOM. Part II: climate variability. *Climate Dyn.*, **50**, 2369-2394, doi:10.1007/s00382-016-3192-6.

Rackow, T., D. V Sein, T. Semmler, S. Danilov, N. V. Koldunov, D. Sidorenko, W. Wang, and T. Jung, 2019: Sensitivity of deep ocean biases to horizontal resolution in prototype CMIP6 simulations with AWI-CM1.0. *Geosci. Model Dev.*, **12**, 2635-2656, doi:10.5194/gmd-12-2635-2019.

Rahaman, H., and Coauthors, 2020: An assessment of the Indian Ocean mean state and seasonal cycle in a suite of interannual CORE-II simulations. *Ocean Modell.*, **145**, 101503, doi:10.1016/j.ocemod.2019.101503.

Renault, L., J. McWilliams, P. Penven, 2017: Modulation of the Agulhas current retroflection and leakage by oceanic current interaction with the atmosphere in coupled simulations. *J. Phys. Oceanogr.,* **47**, 2077–2100, doi:10.1175/JPO-D-16-0168.1.

Renault, L., S. Masson, T. Arsouze, G. Madec, and J. C. McWilliams, 2019: Recipes for how to force oceanic model dynamics, *J. Adv. Model. Earth Syst.*, **11**, doi:10.1029/2019MS001715.

Richardson, P. L., 1993: A census of eddies observed in North Atlantic SOFAR float data. *Prog. Oceanogr.*, **31**, 1–50, doi:10.1016/ 0079-6611(93)90022-6.

Rio, M.-H., S. Mulet, and N. Picot, 2014: Beyond GOCE for the ocean circulation estimate: Synergetic use of altimetry, gravimetry, and in situ data provides new insight into geostrophic and Ekman currents. *Geophys. Res. Lett.*, **41**, 8918–8925, doi:10.1002/2014GL061773.

Rossby, T., 1996: The North Atlantic Current and surrounding waters: At the crossroads. *Rev. Geophys.*, **34**, 463– 481, doi:10.1029/96RG02214.

Sein, D. V., S. Danilov, A. Biastoch, J. V. Durgadoo, D. Sidorenko, S. Harig, and Q. Wang, 2016: Designing variable ocean model resolution based on the observed ocean variability. *J. Adv. Model. Earth Syst.*, **8**, 904-916, doi:10.1002/2016MS000650.

Sein, D. V., and Coauthors, 2018: The relative influence of atmospheric and oceanic model resolution on the circulation of the North Atlantic Ocean in a coupled climate model. *J. Adv. Model. Earth Syst.*, **10**, 2026-2041. doi:10.1029/2018MS001327.

Sidorenko, D., and Coauthors, 2015: Towards multi-resolution global climate modeling with ECHAM6-FESOM. Part I: Model formulation and mean climate. *Climate Dyn.*, **44**, 757-780, doi:10.1007/s00382-014-2290-6.

Sidorenko, D., and Coauthors, 2018: Influence of a salt plume parameterization in a coupled climate model. *J. Adv. Model. Earth Syst.*, **10**, 2357-2373, doi:10.1029/2018MS001291.

Tseng, Y., and Coauthors, 2016: North and equatorial Pacific Ocean circulation in the CORE-II hindcast simulations. *Ocean Modell.*, **104**, 143–170, doi:10.1016/j.ocemod.2016.06.003.

Tsujino, H., and Coauthors, 2018: JRA-55 based surface dataset for driving ocean-sea-ice models (JRA55-do). *Ocean Modell.*, **130**, 79–139, doi:10.1016/j.ocemod.2018.07.002.

Tsujino, H., and Coauthors, 2020: Evaluation of global ocean-sea-ice model simulations based on the experimental protocols of the Ocean Model Intercomparison Project phase 2 (OMIP-2). *Geo. Model. Dev.*, Submitted.

Wang, Q., and Coauthors, 2016a: An assessment of the Arctic Ocean in a suite of interannual CORE-II simulations. Part I: Sea ice and solid freshwater. *Ocean Modell.*, **99**, 110–132, doi:10.1016/j.ocemod.2015.12.008.

Wang, Q., and Coauthors, 2016b: An assessment of the Arctic Ocean in a suite of interannual CORE-II simulations. Part II: Liquid freshwater. *Ocean Modell.*, **99**, 86-109, doi:10.1016/j.ocemod.2015.12.009.

Yu, Y. Q., S. L. Tang, H. L. Liu, P. F. Lin, and X. L. Li, 2018: Development and evaluation of the dynamic framework of an ocean general circulation model with arbitrary orthogonal curvilinear coordinate. *Chin. J. Atmos. Sci.*, **42**, 877-889, doi:10.3878/j.issn.1006-9895.1805.17284.

Yu, Z. P., H. L. Liu, and P. F. Lin, 2017: A numerical study of the influence of tidal mixing on Atlantic meridional overturning circulation (AMOC) simulation. *Chin. J. Atmos. Sci.*, **41**, 1087−1100, doi:10.3878/j.issn.1006-9895.1702.16263.

Zhang, X. H., and X. Liang, 1989: A numerical world ocean general circulation model. A*dv. Atmos. Sci.*, **6**, 43-61, doi:10.1007/BF02656917.

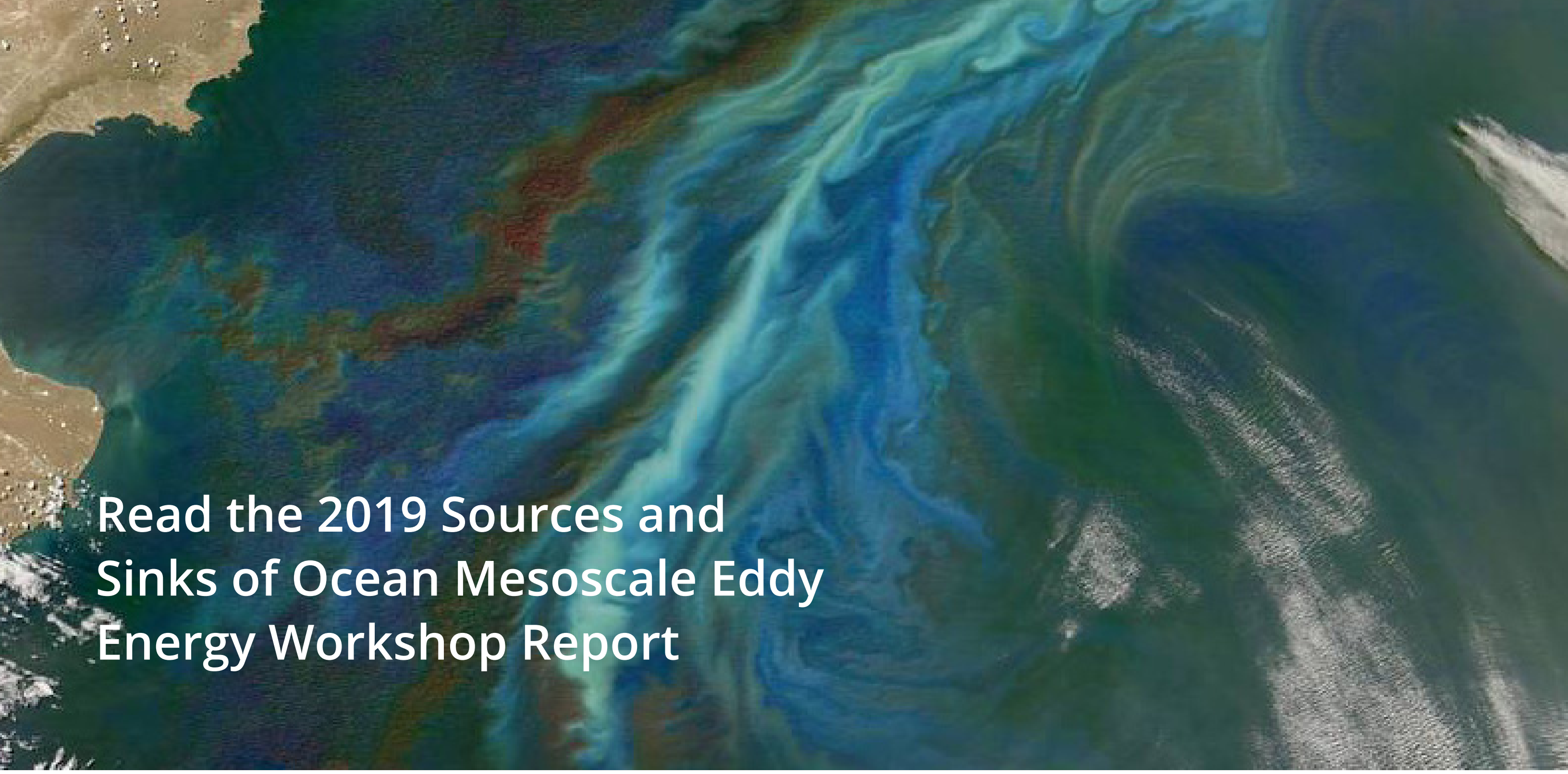

# Read the 2019 Sources and Sinks of Ocean Mesoscale Eddy Energy Workshop Report

*Image credit: NASA Earth Observatory*


**International CLIVAR Project Office**
First Institute of Oceanography, MNR,
6 Xianxialing Road, Laoshan District, Qingdao
266061,China
icpo@clivar.org
http://www.clivar.org
twitter.com/wcrp_clivar

**US CLIVAR Project Office**
1201 New York Ave. NW, Suite 400
Washington, DC 20005
(202) 787-1682
uscpo@usclivar.org
www.usclivar.org
twitter.com/usclivar


CLIVAR is the World Climate Research Programme's (WCRP) core project on the ocean-atmosphere system.

World Climate Research Programme


WCRP is sponsored by the World Meteorological Organization, the Intergovernmental Oceanographic Commission of UNESCO, and the International Science Council. The ICPO is supported by Ministry of Natural Resources of the People's Republic of China/ First Institute of Oceanography (FIO) and the Indian Ministry of Earth Sciences/ Indian Institute of Tropical Meteorology (IITM).

US CLIVAR acknowledges support from these US agencies:

This material was developed with federal support of NASA (80NSSC17M0007), NOAA (NA11OAR4310213), NSF (AGS-1502208), and DOE (DE-SC0016332). Any opinions, findings, conclusions, or recommendations expressed in this material are those of the authors and do not necessarily reflect the views of the sponsoring agencies.